

PAPER • OPEN ACCESS

Thermal transmittance prediction based on the application of artificial neural networks on heat flux method results

To cite this article: S. Gumbarević *et al* 2021 *J. Phys.: Conf. Ser.* **2069** 012152

View the [article online](#) for updates and enhancements.

You may also like

- [Enhanced-recycling H-mode regimes with edge coherent modes achieved by RF heating with lithium-wall conditioning in the EAST superconducting tokamak](#)
H.Q. Wang, G.S. Xu, H.Y. Guo et al.
- [The design, fabrication and characterization of fluidic membranes for micro-engines with the aim of frequency lowering](#)
R Chutani, F Formosa, M de Labachellerie et al.
- [Macroscopic effects in generation of attosecond XUV pulses via high-order frequency mixing in gases and plasma](#)
V A Birulia, M A Khokhlova and V V Strelkov



ECS
The
Electrochemical
Society
Advancing solid state &
electrochemical science & technology

DISCOVER
how sustainability
intersects with
electrochemistry & solid
state science research

Thermal transmittance prediction based on the application of artificial neural networks on heat flux method results

S. Gumbarević, B. Milovanović, M. Gaši and M. Bagarić

University of Zagreb, Faculty of Civil Engineering, Department of Materials, Fra Andrije Kačića Miošića 26, 10000 Zagreb, Croatia

E-mail: sanjin.gumbarevic@grad.unizg.hr, bojan.milovanovic@grad.unizg.hr, mergim.gasi@grad.unizg.hr, marina.bagaric@grad.unizg.hr

Abstract. Deep energy renovation of building stock came more into focus in the European Union due to energy efficiency related directives. Many buildings that must undergo deep energy renovation are old and may lack design/renovation documentation, or possible degradation of materials might have occurred in building elements over time. Thermal transmittance (i.e. U-value) is one of the most important parameters for determining the transmission heat losses through building envelope elements. It depends on the thickness and thermal properties of all the materials that form a building element. In-situ U-value can be determined by ISO 9869-1 standard (Heat Flux Method – HFM). Still, measurement duration is one of the reasons why HFM is not widely used in field testing before the renovation design process commences. This paper analyzes the possibility of reducing the measurement time by conducting parallel measurements with one heat-flux sensor. This parallelization could be achieved by applying a specific class of the Artificial Neural Network (ANN) on HFM results to predict unknown heat flux based on collected interior and exterior air temperatures. After the satisfying prediction is achieved, HFM sensor can be relocated to another measuring location. Paper shows a comparison of four ANN cases applied to HFM results for a measurement held on one multi-layer wall – multilayer perceptron with three neurons in one hidden layer, long short-term memory with 100 units, gated recurrent unit with 100 units and combination of 50 long short-term memory units and 50 gated recurrent units. The analysis gave promising results in term of predicting the heat flux rate based on the two input temperatures. Additional analysis on another wall showed possible limitations of the method that serves as a direction for further research on this topic.

1. Introduction

The building sector is recognized as an area where action can be taken through energy efficiency regulations to reduce humanity's impact on the environment [1], it is clear that there is a significant need for energy retrofitting of the building stock [2]. One of the most important criteria to increase the energy efficiency of a building is to limit the thermal transmittance (U-value) of a particular building element. It is a great challenge to estimate the U-value of the envelope element of an existing building [3, 4] due to the possible deterioration of the thermal properties of the layers forming the element, the influence of heterogeneity in the element, the influence of moisture in the element [5, 6] and information loss for element materials and its properties. Therefore, in case of such assessment, it is more reasonable to use some experimental



Content from this work may be used under the terms of the [Creative Commons Attribution 3.0 licence](https://creativecommons.org/licenses/by/3.0/). Any further distribution of this work must maintain attribution to the author(s) and the title of the work, journal citation and DOI.

method to determine element's U-value in existing buildings. One of common used is heat flux method (HFM) and it is standardized according to ISO 9869-1 [7], which uses a sensor to measure heat flux and two thermocouples to measure indoor and outdoor air temperatures. Based on the measured two temperatures and one heat flux, the U-value is estimated using one of the two proposed standardized methods – from the average of the measured quantities (steady-state method) or using transformations of the heat conduction equation (dynamic method) [3, 8]. In order for the results of the field test to be relevant, it is necessary to perform the test when the element is located at the boundary between the internal and external environment under conditions with a high temperature gradient [9]. If these conditions are not present, then there is a high probability of obtaining a significant deviation with respect to the designed U-value [10]. When these conditions are met, the maximum deviation of the HFM result is usually limited to a maximum value of about 20% of the difference between the designed and field U-values [11, 12]. The reliability of HFM results is also affected by climate conditions of the external environment (rain, sun) and large temperature variations [13]. It is especially important to keep the internal boundary condition as close as possible to a constant value [14]. Moreover, the main disadvantage of HFM is the duration of the test, which can be extended to 2 weeks if the criteria of the standard are met [3, 13, 14]. The reliability of the estimated U-value is significantly increased when the dynamic method is used in the post-processing of the results [15, 16], since for the six analyzed cases in [16] there is a difference of about 10% compared to the designed U-value when using the steady-state method, and this difference when using the dynamic method does not exceed 3%. When using the dynamic method, it is possible to reduce the testing time by one or two days if we consider the three analyzed cases in [17], but the measurement can still take up to 7 days. Since the boundary conditions are difficult to handle, as the external boundary condition is the outside air temperature and the internal one is the constant room temperature [14], the test time of several different building elements can be reduced either by using multiple HFM sensors (which is financially and operationally inefficient [18]) or by evaluating the sensor results according to the assumed behavior pattern. Such prediction of sensor results is potentially possible with artificial intelligence [19].

2. Methodology

Methods and instruments used in this research can be classified in two groups – methods and instruments for data collection and methods for data prediction. For data collection, HFM is used for collection of internal and external air temperatures as well as heat flux through specialized sensor. HFM is deeply explained in section 2.1. For data analysis and prediction, artificial neural network methods are used and they are explained in section 2.2.

2.1. Heat flux method

HFM is standardized method for measuring heat flux through the building element and for estimating the field U-value based on measured parameters. HFM instrument kit that is used in the research is gSKIN®Heat Flux Sensor (Table 1).

The goal of this research is to calculate the U-value using several ANN models and to find one that has the best performance in a compare to the U-value calculated using the average method defined in the ISO 9869-1 standard [7] (1):

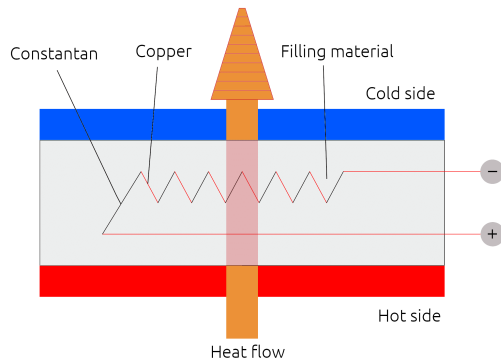
$$U = \frac{\sum_{j=1}^N q_j}{\sum_{j=1}^N (T_i - T_e)_j}, \quad (1)$$

where T_i and T_e are the internal and external air temperatures, respectively, and q is the heat flow rate. Index j is corresponding to the measurement data point.

Table 1. Heat flux kit specifications - heat flux sensors and 2 thermocouples.

Model	gSKIN®Heat Flux Sensor
Sensitivity	10.93 μ V/(W/m ²)
Correction factor	0.0137 [μ V/(W/m ²)]/°C
Dimensions	30.0 × 30.0 mm
Thickness	2.0 mm
Electrical resistance at 22.5 °C	≤100 Ω
Relative error	±3%
Temperature range	−50 °C / +150 °C

The heat flux sensor is an instrument which measures a heat flow passing through it by producing an electrical signal which is a linear function of the heat flow. These sensors are usually flat, thermally resistive plates (schematically shown in Figure 1.) with thermocouples that have several thermophiles integrated inside of the thermocouple substrate.

**Figure 1.** Schematic cross section through heat flux meter.

2.2. Artificial neural networks

Area of artificial intelligence and machine learning (ML) started to be used significantly in the last decade due to development of faster computer machines and engagement of new learning algorithms [20]. Large part of ML models depend on the concept of ANN. ANN is briefly a systematical set of weighting coefficients, biases and activation functions, and they behave as one function which transforms input variables to output ones with a goal to predict an outcome as close as possible to target values [21]. The most simple and firstly developed class of ANN is multilayer perceptron (MLP), schematically presented on figure 2. ANN model from figure 2 is relatively simple and has two variables in the input layer, three neurons in hidden layer, and one output variable. Type of ANN model that has one output variable is called regression model compared to ANN model that has more outputs - classification model. The logic behind those two is the same, input variables are connected to neurons in hidden layers with functions that multiply each input and add a bias to it. In each neuron i in hidden layer n , summation $z_i^{(n)}$ of transformed inputs is performed (2) and transformation of this summation with the activation function $\varphi_{n,i}$ (3) where m is the number of inputs into neuron, $w_{0,n}^{(n)}$ is bias, $w_{j,i}^{(n)}$ is weighting coefficient and y_i^n is value that is passed to the next layer, $n + 1$.

$$z_{n,i} = w_{0,i}^{(n)} + \sum_{j=1}^m x_j w_{j,i}^{(n)} \quad (2)$$

$$y_{n,i} = \varphi_{n,i}(z_{n,i}) \quad (3)$$

For the last layer N , i.e. output layer, and if we have only one variable \hat{q} , the predicted value is described with equation (4).

$$\hat{q} = w_0^{(N)} + \sum_{j=1}^{m_{N-1}} \varphi_j^{N-1}(z_{N-1,j}) w_j^{(N)} \quad (4)$$

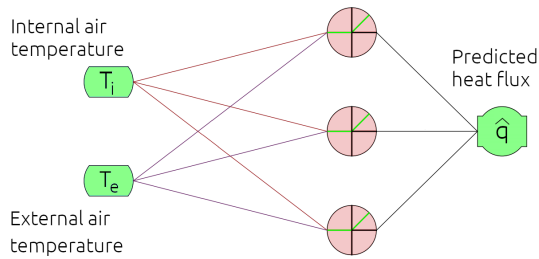


Figure 2. Multilayer perceptron class of artificial neural network with two inputs, three neurons in hidden layer, and one output.

Activation function is a nonlinear function which decides how much information is passed through each neuron to the next layer of neurons, and in this way information is carried from input layer through neurons in hidden layers all the way to output layer neurons. The most common activation functions are *sigmoid*, *tanh* and *ReLU*.

ANN can learn by comparing predicted variables with actual ones. Firstly, it is essential to define loss $\mathcal{L}(f(x^{(i)}; \mathbf{W}), y^{(i)})$ between predicted $f(x^{(i)}; \mathbf{W})$ and actual $(y^{(i)})$ variables where \mathbf{W} is matrix of weighting coefficients and biases. The empirical loss (5) can then be defined as total loss over the entire dataset. This is performed iteratively using the gradient method (often optimized) by computing the gradient $\frac{\partial J(\mathbf{W})}{\partial \mathbf{W}}$ and by updating the weights matrix \mathbf{W} until convergence is achieved.

$$J(\mathbf{W}) = \frac{1}{n} \sum_{i=1}^n \mathcal{L}(f(x^{(i)}; \mathbf{W}), y^{(i)}) \quad (5)$$

For regression problems, loss function \mathcal{L} is usually mean squared error function. The "learning" is performed with minimization of empirical loss on network weights to obtain a matrix \mathbf{W}^* with weighting coefficients that achieve the lowest loss (6).

$$\mathbf{W}^* = \underset{\mathbf{W}}{\operatorname{argmin}} \frac{1}{n} \sum_{i=1}^n (y^{(i)} - f(x^{(i)}; \mathbf{W}))^2 \quad (6)$$

For time series regression problems, another ANN class is commonly used – recurrent neural networks (RNN). The reason for this is that RNN depend not only on input entry in certain timestep, but also on value from previous cell state. Two types of RNN were analyzed in the paper – long-short term memory (LSTM) [22] cells and gated recurrent units (GRU) [23]. Those two consist of set of gates that transform the inputs and previous cell states to provide outputs and transformed information that goes to the next cell. LSTM unit consists of four gates (figure 3): forget gate f_t to forget irrelevant parts of the previous cell state, store gate i_t for storing relevant new information into cell state, update for selective update of cell state values and output gate o_t that controls what information is sent to the next timestep.

GRU has one gate less than LSTM (it does not have forget gate) and schematic view of it can be seen in figure 4. It consists of reset gate r_t , update gate z_t and candidate activation gate \tilde{h}_t . Although they look slightly different, RNN follow the same principles described for MLP.

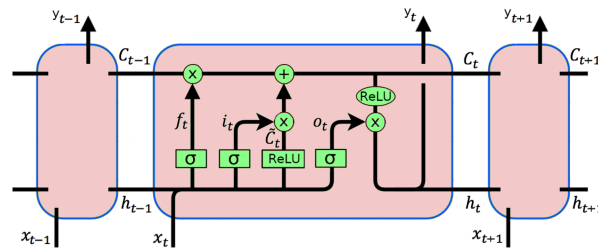


Figure 3. Schematic view of long-short term memory unit with ReLU activation function.

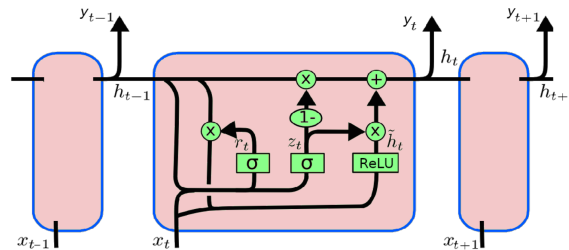


Figure 4. Schematic view of gated recurrent unit with ReLU activation function.

2.3. Research design

HFM experiment with instrumentation described in section 2.1 and according to ISO 9869-1 standard [7] was carried out on a wall with unknown U-value in the period between 22 February 2019 and 26 February 2019 (figure 5). Experimental data that is analyzed consists of 490 data entries collected every 10 minutes (in total 81.67 hours). In each time step, three values were measured – internal and external air temperatures with thermocouples and heat flux with heat flux sensor. Prediction of heat flux is performed with four ANN architectures.

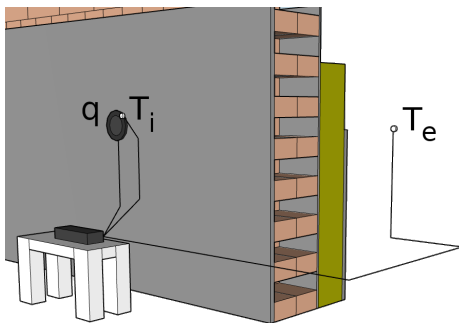


Figure 5. Experimental setup for HFM data acquisition for analyzed wall.

Four types of ANN architectures were analyzed: MLP3 – multilayer perceptron with 3 neurons in hidden layer, LSTM100 – architecture with 100 LSTM cells in hidden layer, GRU100 – architecture with 100 GRU cells in hidden layer and LSTMGRU100 – architecture with 50 LSTM cells in first hidden layer and 50 GRU cells in second hidden layer. Three cases of train/validation ratios were observed for each architecture: 1/4, 1/2 and 2/3. Results of predicted U-values were compared to the measured U-value. Predicted U-values were calculated in accordance with expression (1) applied on predicted results of heat flux. Point of interest was predicted sequence based on trained ML model. Comparison between predicted and true sequences was described by root mean squared error (RMSE), mean squared error (MSE) and mean absolute error (MAE).

3. Results

Table 2 shows information described in previous subsection with pointing up the best accuracy for certain train/validation ratio taking concern RMSE.

Table 2. Results comparison of four types of ANN architectures. Prediction of heat flux (RMSE, MSE, MAE) and U-values – prediction v.s. measured $0.586 \text{ W}/(\text{m}^2 \text{ K})$.

ANN type	train/validation	RMSE	MSE	MAE	predicted U-value	rel. difference
MLP3	1/4	2.02*	4.06	1.44	0.534	8.96%
	1/2	2.14	4.58	1.55	0.574	2.23%
	2/3	1.91	3.63	1.41	0.546	7.03%
LSTM100	1/4	4.36	19.04	3.19	0.615	4.72%
	1/2	1.68*	2.82	1.14	0.556	5.31%
	2/3	1.52	2.31	1.03	0.546	6.99%
GRU100	1/4	2.65	7.03	1.95	0.571	2.67%
	1/2	1.77	3.13	1.23	0.594	1.30%
	2/3	1.45	2.10	0.92	0.548	6.66%
LSTMGRU100	1/4	2.88	8.31	1.98	0.573	2.30%
	1/2	2.02	4.08	1.22	0.605	3.02%
	2/3	1.22*	1.48	0.68	0.563	4.13%

* the best accuracy for certain train/validation ratio

If we observe training/validation ratio 1/4, the best matching is registered for MLP3 ANN architecture with RMSE 2.02 which can be seen in table 2. Predictions from all analyzed ANN architectures for this case is shown in figure 6 and comparison of MLP3 predicted to actual (measured) values in figure 7. Vertical line is boundary between training and validation data. For training/validation ratios 1/2 and 2/3, better results were achieved as shown in table 2 and on figures 8 and 9.

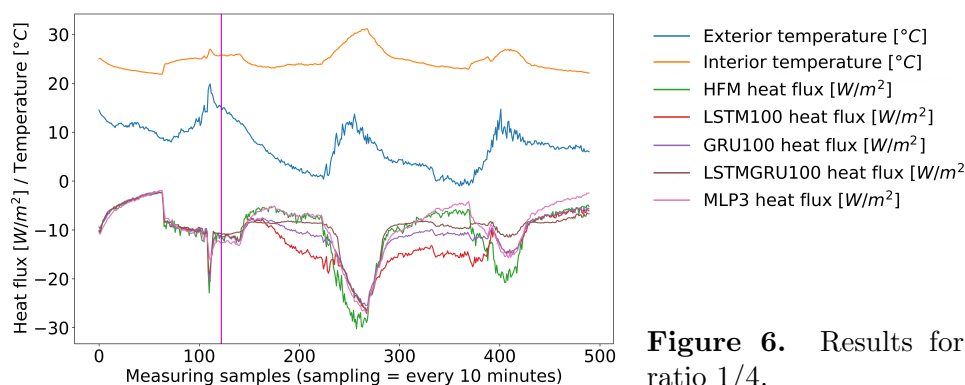


Figure 6. Results for training/validation ratio 1/4.

The best result is achieved for ANN architecture LSTMGRU100 for training/validation ratio 2/3 but it is probably because training part is 2/3 of whole dataset. More valuable result is for training/validation ratio 1/2 – for ANN architecture LSTM100. RMSE for this ML model is 1.68 and relative difference when comparing to measured U-value is 5.31%.

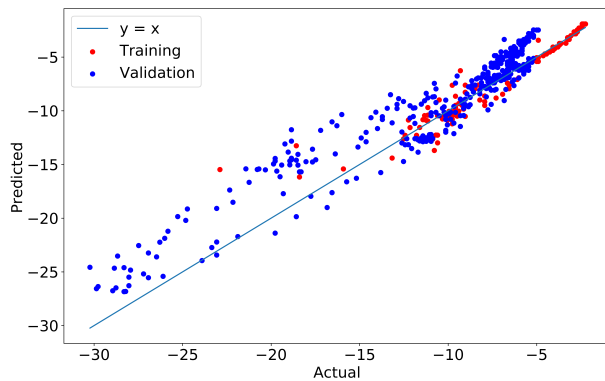


Figure 7. Predicted vs. actual heat flux for MLP3 for training/validation ratio 1/4.

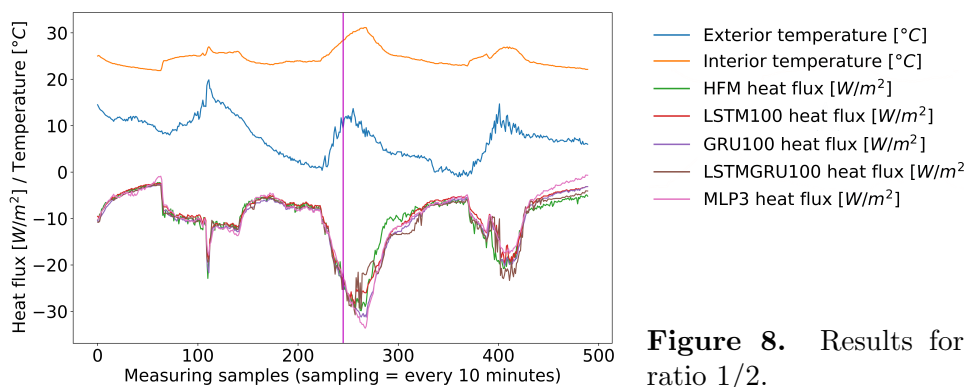


Figure 8. Results for training/validation ratio 1/2.

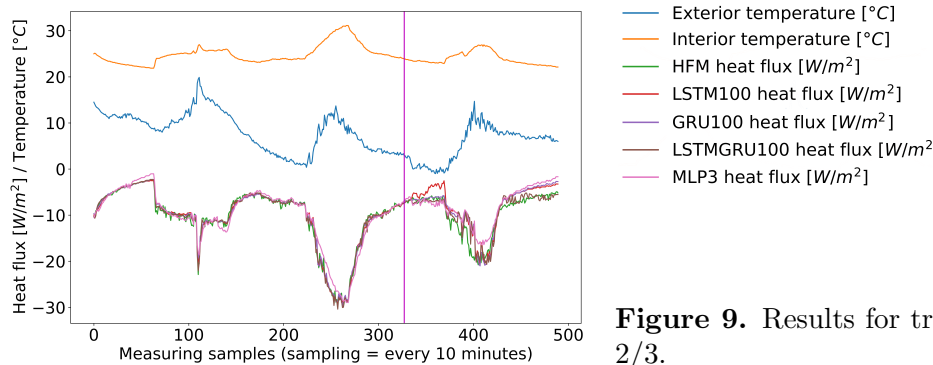


Figure 9. Results for training/validation ratio 2/3.

4. Discussion and conclusion

The results are promising in terms of prediction of heat flux based on measured heat flux with two input temperatures in training period, and after the training period by measuring just input temperatures. Results show that RNN architectures give reliable results for larger dataset used for training (1/2 and 2/3 training/validation ratios) while MLP is better for smaller training dataset. This should be deeply analyzed because the goal is to reliably predict HFM results with small amount of data, but this prediction must be stable. MLP could not provide stability because it is not as nonlinear as RNN architectures so it might not reliably predict the HFM results in the long-run.

The most noticeable limitation of the method could be an influence by a change in the boundary temperatures in a way it is not observed in ML training period. E.g. for wall in figure 10 it can be seen that after the training is done on 1/4 of total dataset, prediction is stable until such kind of change (red-marked in figure 10). This can be solved by defining

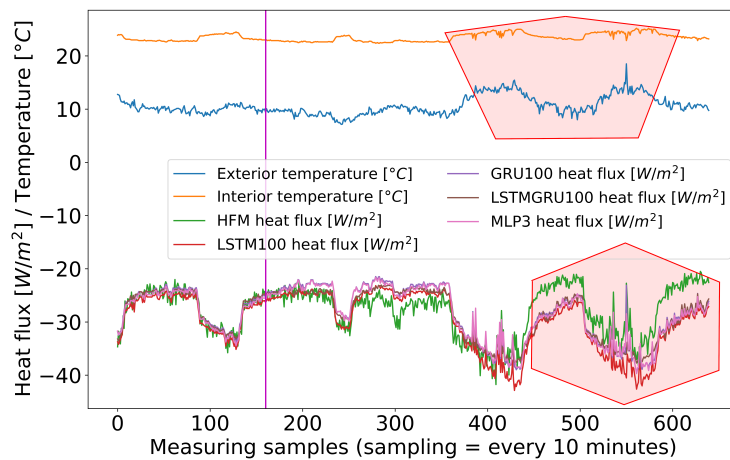


Figure 10. Analysis on additional wall with red-mark describing possible cause of non-stable prediction.

strict measuring conditions and/or by applying regularization techniques. For more certain conclusions, additional experimental investigation and analysis should be carried out.

Acknowledgments

One of the authors (Sanjin Gumbarević) would like to acknowledge the Croatian Science Foundation and European Social Fund for the support under the project ESF DOK-01-2018.

References

- [1] Laaroussi Y, Bahrar M, Zavrl E, Mankibi M E and Stritih U 2020 *Sustainable Cities and Society* **63** 102452
- [2] Jensen P A, Maslesa E, Berg J B and Thuesen C 2018 *Building and Environment* **143** 130–137
- [3] Bienvenido-Huertas D, Moyano J, Marín D and Fresco-Contreras R 2019 *Renewable and Sustainable Energy Reviews* **102** 356–371
- [4] Ficco G, Iannetta F, Ianniello E, d'Ambrosio Alfano F R and Dell'Isola M 2015 *Energy and Buildings* **104** 108–121
- [5] Gomes M G, Flores-Colen I, Manga L, Soares A and de Brito J 2017 *Construction and Building Materials* **135** 279–286
- [6] Lucchi E 2017 *Energy and Buildings* **151** 393–405
- [7] International Organization of Standardization ISO 9869-1:2014 – Thermal insulation. Building elements. In-situ measurement of thermal resistance and thermal transmittance. Heat flow meter method Tech. rep.
- [8] Soares N, Martins C, Gonçalves M, Santos P, da Silva L S and Costa J J 2019 *Energy and Buildings* **182** 88–110
- [9] Bienvenido-Huertas D 2020 *Sustainability* **12** 6247
- [10] Tejedor B, Gaspar K, Casals M and Gangoellis M 2020 *Applied Sciences* **10** 8337
- [11] Evangelisti L, Guattari C and Asdrubali F 2019 *Energy and Buildings* **203** 109441
- [12] Rezvani F, and Bribián I Z 2019 *Revista de la construcción* **18** 311–322
- [13] Meng X, Luo T, Gao Y, Zhang L, Shen Q and Long E 2017 *Applied Thermal Engineering* **122** 747–757
- [14] Roque E, Vicente R, Almeida R M, da Silva J M and Ferreira A V 2020 *Applied Thermal Engineering* **169** 114935
- [15] Gaši M, Milovanović B and Gumbarević S 2019 *Buildings* **9** 132
- [16] Choi D S and Ko M J 2017 *Energies* **10** 1019
- [17] Gaspar K, Casals M and Gangoellis M 2018 *Energy and Buildings* **176** 360–370
- [18] Márquez J M A, Bohórquez M A M and Melgar S G 2017 *Sensors* **17** 2017
- [19] Gumbarević S, Milovanović B, Gaši M and Bagarić M 2020 *Proceedings of 7th International Electronic Conference on Sensors and Applications (MDPI)*
- [20] Jordan M I and Mitchell T M 2015 *Science* **349** 255–260
- [21] Amini A and Soleimany A 2021 *Massachusetts Institute of Technology: MIT OpenCourseWare*, <https://ocw.mit.edu>. License: Creative Commons BY-NC-SA.
- [22] Hochreiter S and Schmidhuber J 1997 *Neural Computation* **9** 1735–1780
- [23] Cho K, van Merriënboer B, Gulcehre C, Bahdanau D, Bougares F, Schwenk H and Bengio Y 2014 (*Preprint* 1406.1078)